

Effects of Competition in the Stabilization of Point Defects

M. Israeli, N. Kristianpoller, and R. Chen

Department of Physics and Astronomy, Tel-Aviv University, Tel-Aviv, Israel

(Received 3 April 1972)

The dependence of the number of point defects on the dose and on the wavelength of the exciting radiation has been studied in uv-irradiated alkali halides. The existence of various types of traps for the stabilization of defects and the occurrence of competition between these traps were assumed. Theoretical expressions were derived for the number of defects induced by the monochromatic uv radiation. These expressions were found to agree with the experimentally measured dose dependences, as well as the thermoluminescence excitation spectra. They included various previously derived functions as special cases. The observed superlinear dose dependence of the intensities of most glow peaks in NaCl is explained by the proposed mechanism.

I. INTRODUCTION

In recent work, processes of defect formation by ionizing and nonionizing uv light have been studied by thermoluminescence (TL) methods.¹ The relatively high sensitivity of TL measurements compared with absorption measurements enabled the use of monochromatic uv light for excitation. The excitation spectra of the glow peaks and the dependence of their intensities on the dose of the exciting radiation revealed relevant information concerning the mechanism of defect creation.

Different processes were found to be responsible for the excitation of TL.² One process was dominant in the case of irradiation in the spectral region of the band-to-band transitions and the other was dominant mainly by irradiation in the region of the exciton bands. The process responsible for the latter case was found to fit the excitonic mechanism proposed by Hersh and by Pooley,³ while the former was found to be connected with the creation of V_k centers. In each of these cases, an absorbed photon caused the creation of a stable pair of defects (a Frenkel pair or a pair which consisted of a V_k center and a trapped electron). Glow peaks appeared as a result of the thermal release of one of the constituents of the pair and its recombination with the other.

Assuming a simplified case where only one type of trap was responsible for the stabilization of the defects, expressions for the number of point defects created by the uv irradiation were derived as functions of the radiation dose. These expressions were derived taking into account the absorption coefficient of the crystal and therefore the penetration depth of the exciting monochromatic light. Good agreement with the experimental results was found. The above-mentioned simplified model could not explain, however, the superlinear dose dependence which was detected in certain glow peaks.⁴

In the present work, the superlinear dose de-

pendence is investigated and the mechanism of defect production and TL excitation is studied under more general conditions. Expressions for the kinetics of these processes are developed, taking into account the existence of various traps for the stabilization of defects and the possibility of competition between these traps.

II. THEORY

It is assumed that pairs of defects are created in the crystal by uv irradiation, and that the creation rate of these pairs is proportional to the photon flux (s) of the incident monochromatic radiation, and also to the absorption coefficient (μ). The constituents of a pair which do not recombine immediately upon creation may be stabilized. It is considered that one of the constituents (later referred to as defect A) is stabilized in a very short time, in a certain configuration specific to the type of the pair (e. g., the F center in the case of the creation of a Frenkel pair, or the V_k center in the case of creation of a free-electron-hole pair). The second constituent of the pair (later referred to as defect B) is assumed to remain mobile for a relatively longer period of time and may then either be trapped or recombine with a defect of type A . The possibility of the existence of several types of traps (T_i) for the mobile constituent B is presumed. Since these various traps may, generally, have different trapping probabilities (β_i) and may appear in different concentrations (m_i), competition between the traps has to be considered.

Based on these assumptions, the kinetics can be described by the following set of equations:

$$\frac{dn_a}{dt} = \sigma \mu s - \alpha n_a n_f, \quad (1)$$

$$\frac{dm_i}{dt} = -\beta_i m_i n_f, \quad i = 1, 2, \dots \quad (2)$$

$$\frac{dn_f}{dt} = \frac{dn_a}{dt} + \sum_i \frac{dm_i}{dt}, \quad (3)$$

where n_a represents the concentration of the stabilized defects of type A ; n_f is the concentration of the defects of type B , which are free at time t ; and α is the probability for a free defect B to recombine with a stabilized defect A .

Equation (1) gives the time dependence of the density of the stabilized defects A , $\sigma\mu s$ represents the rate of pairs generated by the radiation and the second term represents the rate of recombination. Equation (2) describes the change in the densities of the various unoccupied traps at which defects of type B may be trapped. Equation (3) expresses the consequent changes in the concentration of the free defects B .

Substitution of (1) and (2) into (3) give

$$\frac{dn_f}{dt} = \sigma\mu s - \left(\alpha n_a + \sum_i \beta_i m_i \right) n_f. \quad (4)$$

If T_k and T_l are two different types of traps, elimination of n_f from Eq. (2) leads to

$$\frac{dm_k/dt}{\beta_k m_k} = \frac{dm_l/dt}{\beta_l m_l}. \quad (5)$$

Integrating this equation results in

$$(m_k/m_{0k})^{1/\beta_k} = (m_l/m_{0l})^{1/\beta_l}, \quad (6)$$

where m_{0i} represent the initial concentrations of the unoccupied T_i ($i = 1, 2, \dots, k, \dots, l, \dots$). The relative occupation y_i of the trap T_i is defined by

$$y_i = (m_{0i} - m_i)/m_{0i}. \quad (7)$$

Substituting (7) in (6) gives $(1 - y_k)^{1/\beta_k} = (1 - y_l)^{1/\beta_l}$ and

$$y_k = 1 - (1 - y_l)^{\beta_k/\beta_l}. \quad (8)$$

The "lifetime" of a free defect B is assumed to be very short as compared to the time of irradiation; thus, the rate of the accumulation of free defects can be neglected in comparison with the rate of their annihilation

$$\frac{dn_f}{dt} \ll \left(\alpha n_a + \sum_i \beta_i m_i \right) n_f. \quad (9)$$

Under these conditions we get from Eq. (4)

$$n_f = \frac{\sigma\mu s}{\alpha n_a + \sum_i \beta_i m_i}. \quad (10)$$

Substituting (10) in (1) and (2) leads to

$$\frac{dn_a}{dt} = \frac{\sigma\mu s \sum_i \beta_i m_i}{\alpha n_a + \sum_i \beta_i m_i} \quad (11)$$

and

$$\frac{dm_j}{dt} = - \frac{\sigma\mu s \beta_j m_j}{\alpha n_a + \sum_i \beta_i m_i}, \quad j = 1, 2, \dots \quad (12)$$

From these equations, we have

$$\frac{dn_a}{dt} = - \sum_j \frac{dm_j}{dt}, \quad (13)$$

and therefore

$$n_a = m_0 - \sum_j m_j, \quad (14)$$

where $m_0 = \sum_j m_{0j}$.

Equation (14) states that the number of stabilized defects A equals the number of trapped defects B . This relation obviously holds for any time except for the very beginning of irradiation.

Substituting (14) into (12) gives

$$\frac{dm_j}{dt} = - \frac{\sigma\mu s \beta_j m_j}{\alpha m_0 + \sum_i (\beta_i - \alpha) m_i}, \quad j = 1, 2, \dots \quad (15)$$

which can also be written as

$$\frac{m_0}{\beta_j} \frac{d}{dt} \ln(m_j) + \sum_i \left(\frac{\beta_i}{\alpha} - 1 \right) \frac{m_i}{\beta_j m_j} \frac{dm_i}{dt} = - \frac{\sigma}{\alpha} \mu s. \quad (16)$$

Taking into account Eq. (5), the expression $(m_i/\beta_j m_j) dm_i/dt$ can be replaced by $(1/\beta_i) dm_i/dt$ and therefore

$$\frac{m_0}{\beta_j} \frac{d}{dt} \ln(m_j) + \sum_i \left(\frac{1}{\alpha} - \frac{1}{\beta_i} \right) \frac{dm_i}{dt} = - \frac{\sigma}{\alpha} \mu s. \quad (17)$$

Integration over the irradiation time t results in

$$- \frac{m_0}{\beta_j} \ln \left(\frac{m_j}{m_{0j}} \right) + \sum_i \left(\frac{1}{\alpha} - \frac{1}{\beta_i} \right) (m_{0i} - m_i) = \frac{\sigma}{\alpha} \mu s t$$

or

$$- b_j \ln(1 - y_j) + \sum_i a_i y_i = C \epsilon D, \quad j = 1, 2, \dots \quad (18)$$

where $a_i = m_{0i}(1/\alpha - 1/\beta_i)$, $b_i = m_0/\beta_i$, $C = \sigma/\alpha L$ (where L is the thickness of the crystal), $\epsilon = \mu L$, and $D = st$.

The radiation dose D at a depth χ from the surface of the crystal is given by

$$D = D_0 e^{-\mu\chi} = D_0 e^{-\epsilon\phi}, \quad (19)$$

where D_0 is the incident radiation dose on the crystal surface and $\phi = \chi/L$. With the help of relations (8) and (19), Eq. (18) is transformed to

$$- b_j \ln(1 - y_j) + a_j y_j + \sum_{i \neq j} a_i [1 - (1 - y_j)^{\beta_i/\beta_j}] = C \epsilon D_0 e^{-\epsilon\phi}, \quad j = 1, 2, \dots \quad (20)$$

Equation (20) expresses the relative occupation y_j of a certain trap T_j as a function of the absorption coefficient, the depth in the crystal, and the incident radiation dose. This function also includes the effects of competition between T_j and all the other traps. The total number of defects B , which are finally trapped at T_j at all points in the crystal, is given by

$$N_j = M_{0j} \int_0^1 y_j(\phi) d\phi, \quad j = 1, 2, \dots \quad (21)$$

where $M_{0j} = V m_{0j}$ (V is the crystal volume).

Examples showing the dependence of N_j on D_0 and ϵ for a case of two types of traps for the free

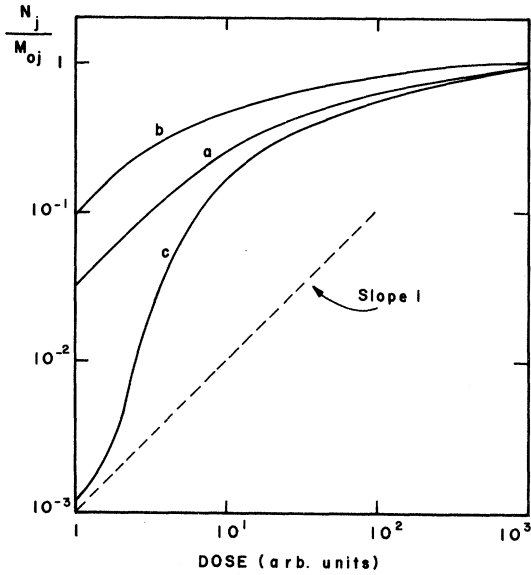


FIG. 1. Theoretical dose dependence of the normalized number of defects stabilized at a single trap, or several traps of equal trapping probabilities (curve a); two competing traps of different trapping probabilities (curve b and c). (The trapping probability in curve b was taken 100 times larger than that in c.)

defects are given in Figs. 1 and 2. For the numerical computation of N_1 and N_2 from Eq. (21), a certain set of values for the parameters $a_1, b_1, a_2,$ and C appearing in Eq. (20) was chosen arbitrarily. The various curves in Fig. 1 describe the dose dependence of

$$\frac{N_j}{M_{0j}} = \int_0^1 y_j(\phi) d\phi, \quad j = 1, 2$$

for a certain value of ϵ and various values of b_2 . Curve a corresponds to a case of equal-trapping probabilities $\beta_1 = \beta_2$ or $b_1 = b_2$; in this case the relation $N_1/M_{01} = N_2/M_{02}$ holds true and curve a represents, therefore, both traps. Curves b and c correspond to a case where β_1 and β_2 differ considerably from each other. The ratio β_2/β_1 was taken in this case to be $\frac{1}{100}$ and it can be seen that the number of occupied traps of both T_1 (curve b) and T_2 (curve c) depends linearly on the radiation dose at the very low dose range. The dose dependence of T_2 becomes superlinear for higher doses, when the "faster" trap T_1 begins to be saturated.

The dependence of N_j/M_{0j} on the absorption coefficient was computed for the same cases taking a constant value of D_0 within the superlinear region. This dependence is shown in Fig. 2. It can be seen that in all of these cases $N_1(\epsilon)$ and $N_2(\epsilon)$ reach maxima for certain values of ϵ and decrease for higher values. The fact that N_j vanishes for $\epsilon = 0$ and $\epsilon \rightarrow \infty$ fits the extreme cases where the radiation is not absorbed by the crystal, or where the

absorption coefficient is very high and the penetration depth tends to zero. In the case of irradiation in a spectral region where the absorption coefficient varies from low to very high values, this dependence on ϵ may cause the excitation maxima to appear not at the absorption peaks, but somewhere on the tail of the absorption bands.

Previous studies on trapping mechanisms dealt mainly with the trapping of defects by a single type of trap, and therefore the effect of competition was ignored. The function given by Eq. (20) includes the trapping of defects by a single type of trap as a special case. In this case the concentration of one type of trap (say, T_1), as well as the probability of a free defect to be trapped by T_1 , has to be taken much greater than those of the other traps together. These conditions can be expressed by

$$\beta_1 m_1 \gg \sum_{i \neq 1} \beta_i m_i \tag{22}$$

and

$$m_1 \gg \sum_{i \neq 1} m_i, \tag{23}$$

which leads, obviously, also to $m_{01} \sim m_0$. In this case Eq. (20) reduces to

$$-b_1 \ln(1 - y_1) + a_1 y_1 = C \epsilon D_0 e^{-\epsilon \phi}. \tag{24}$$

The index "1" can now be omitted. Equation (21) therefore becomes

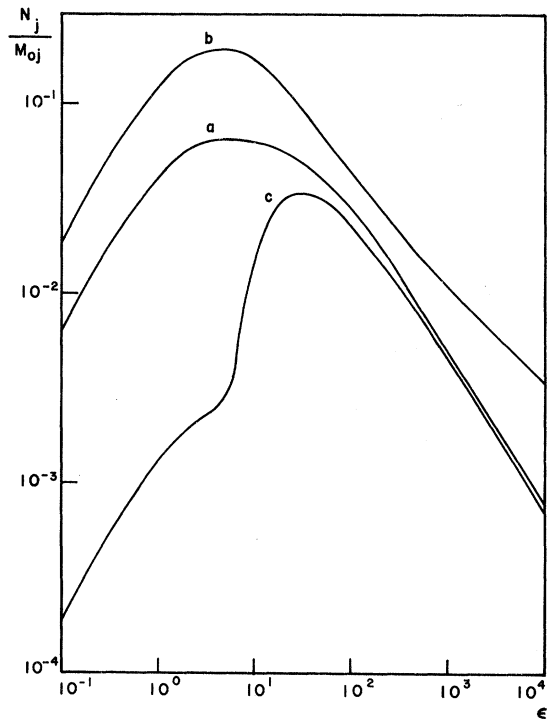


FIG. 2. The normalized number of defects as a function of the absorption coefficient. Curves a-c are as in Fig. 1.

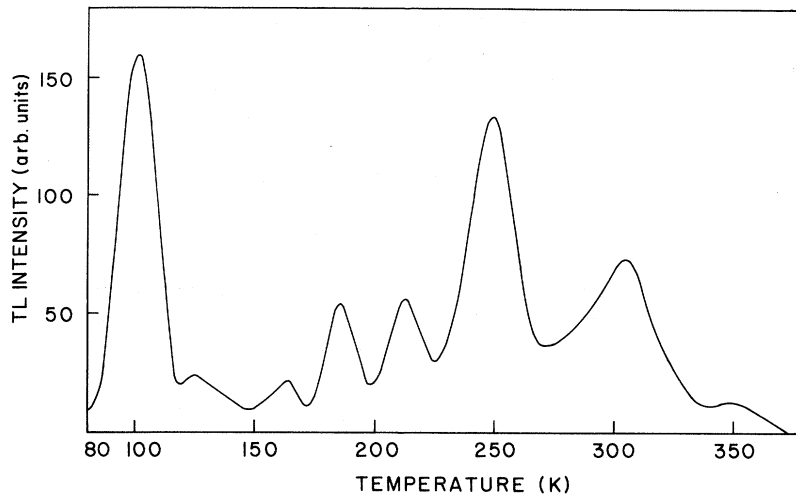


FIG. 3. A typical glow curve of NaCl excited at 80 K by uv light of 160 nm.

$$N = M_0 \int_0^1 y(\phi) d\phi. \quad (25)$$

In fact, curves *a* of Figs. 1 and 2 describe the dependence of N on D_0 and ϵ also in this case of a dominant trap.

If $y \ll 1$ (which means that T is very far from saturation), Eq. (24) becomes by second approximation

$$by + \frac{1}{2}by^2 + ay = C\epsilon D_0 e^{-\epsilon\phi} \quad (26)$$

or

$$y^2 + 2\left(1 + \frac{a}{b}\right)y - \frac{2C\epsilon}{b}D_0 e^{-\epsilon\phi} = 0.$$

Since in our case

$$1 + \frac{a}{b} = 1 + \frac{m\alpha}{m_0} \left(\frac{\beta}{\alpha} - 1\right) \approx \frac{\beta}{\alpha},$$

Eq. (26) can be written as

$$y^2 + 2\frac{\beta}{\alpha}y - \frac{2C\epsilon}{b}D_0 e^{-\epsilon\phi} = 0. \quad (27)$$

It can be seen that this special case fits the one which has previously been treated in detail in the first paper of Ref. 1. It can also be seen that for the case where the probability for recombination (α) is much greater than the probability for trapping (β), the first approximation might be insufficient. In this case, if the linear terms in (27) can be neglected, y as well as N will then be proportional to $D_0^{1/2}$. Such a square-root dose dependence has previously been studied by various authors.⁵

III. EXPERIMENTAL TECHNIQUES AND RESULTS

Pure NaCl crystals were used in all the measurements. Specimens of $11 \times 9 \times 2$ mm³ were cleaved from a single Harshaw crystal. The samples were irradiated at 80 K by monochromatic uv light in the vacuum region. TL was recorded by

heating the crystals to about 500 K at a rate of 25 K/min. Experimental details have previously been described.^{1,2}

Figure 3 shows a typical glow curve of NaCl excited by irradiation at the long-wavelength tail of the first exciton band. The main glow peaks appear at 102, 186, 213, 250, and 303 K. Weaker peaks appear also at 128, 164, and 350 K. The intensities of all glow peaks except for the 303-K peak were found to be reproducible. The intensity of this 303-K peak decreased after repeated measuring cycles of irradiation and subsequent warming up, and reached then a steady level of about half its initial intensity.

The TL excitation spectra were measured while keeping the irradiation time and the incident photon flux constant. The excitation spectra of the glow peaks at 102, 213, and 250 K are given in Fig. 4. The excitation spectrum of the 186-K glow peak was the same as that of the 213-K peak. The dots in Fig. 4 represent the experimentally measured values, while the solid curves give the computed excitation spectra as explained in Sec. IV. The absorption spectrum of the crystal is shown for comparison by the dashed curve *d*.⁶ It can be seen that all these glow peaks have excitation maxima on the long-wavelength tail of the first exciton band. Only the 303-K glow peak could be excited by more energetic photons corresponding to band-to-band transitions, as well as by photons corresponding to the exciton region.²

The dependence of the glow-peak intensities on the dose of the exciting radiation was measured independently for constant photon flux by varying the irradiation time, as well as for constant irradiation time by increasing the exciting photon flux; the same dependence was found in both cases. All glow peaks showed nearly linear dose dependence for relatively low radiation doses. This

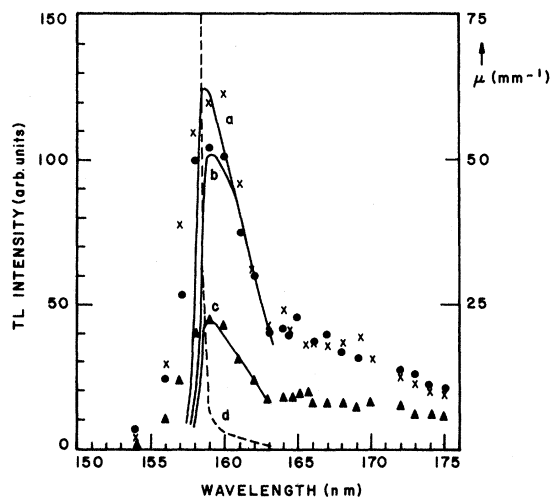


FIG. 4. TL excitation spectra of NaCl excited at 80 K by nonionizing uv light: 102-K (curve a), 250-K (curve b), 213-K glow peaks (curve c). These dots, crosses, and triangles represent the experimentally measured values and the solid curves the theoretical functions. Curve d shows, for comparison, the absorption coefficient of the crystal (data taken from Ref. 6).

linear dependence was followed by a tendency to saturation for higher doses at some of the glow peaks. Examples of such behavior are shown in Fig. 5 on a log-log scale. All these measurements were carried out by excitation with wave-

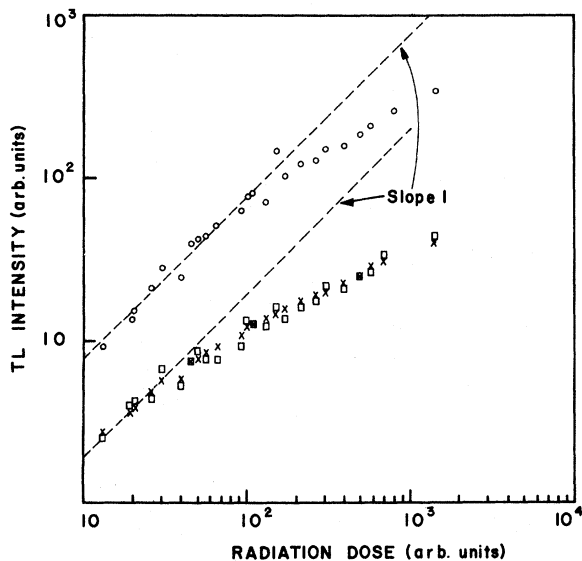


FIG. 5. Experimentally measured dose dependence of the TL intensities of the 303-K (circles) and the 350-K (squares) glow peaks. (Crosses) the computed values of the 350-K glow peak.

length of 160 nm, which corresponds approximately to the maximum of the excitation spectrum. The circles and the squares show the measured values of the 303-K (after reaching steady state) and of the 350-K glow peaks, respectively. The dashed lines are of slope 1, representing a linear dose dependence. All other main glow peaks of NaCl showed, after the initial stage of nearly linear dose dependence, a pronounced superlinear dose dependence. A tendency to saturation appeared also in these glow peaks for relatively high doses. In Fig. 6 the dose dependences of the intensities of the 102-, 213- and 250-K glow peak are given. The experimentally measured values are again represented by dots, while the solid curves show the dose dependences as computed from Eq. (21). The dose dependence of the 186-K glow peak was found to be the same as that of the 213-K peak.

IV. DISCUSSION

The experimental results showed that all glow peaks of NaCl excited by nonionizing uv light had excitation maxima on the long-wavelength tail of the first exciton band. Most of these glow peaks

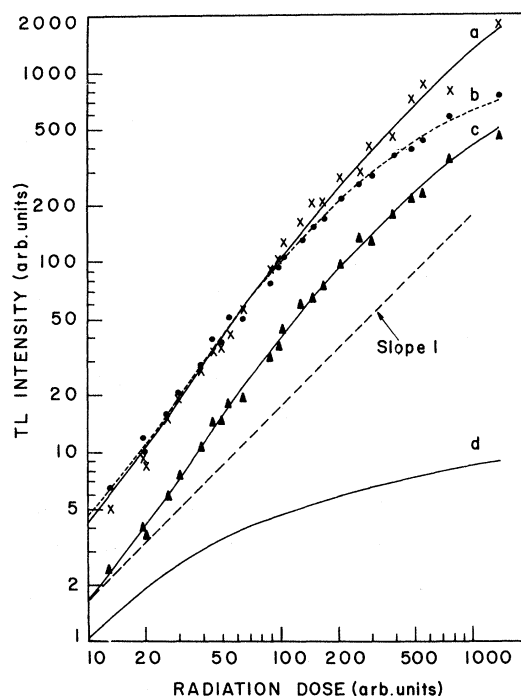


FIG. 6. Dose dependence of the TL intensities of the 102-K (curve a), the 250-K (curve b), and the 213-K glow peaks (curve c). The dots, crosses, and triangles represent the experimentally measured values and the solid curves represent the theoretical functions. Curve d represents the dose dependence of the hypothetically assumed trap (see text).

showed a nearly linear dose dependence for very low doses which became superlinear with increasing doses, and tended toward saturation for higher doses. The theoretical model given in Sec. II predicted in certain cases such behavior for the dependence of the number of radiation-induced defects on the exciting dose and on the absorption coefficient. This model was based on the assumption that pairs of defects are created by the radiation, but no specific assumption was made concerning the type of these defect pairs.

In the present case of uv irradiation into the exciton band, it is supposed that Frenkel pairs are created by an excitonic mechanism. At 80 K, the "free"-halogen interstitials are not stable and may either recombine with an F center or be stabilized by one of the existing traps, which may consist of impurity ions or other imperfections. However, when more than one kind of trap exists, a competition process between the various traps is involved. During the heating of the crystal, the halogen interstitials trapped at different configurations will be released thermally at various temperatures. TL glow peaks may arise as a result of radiative recombination of these freed interstitials with the F centers.

It has recently been shown⁷ that the maximum intensities of these glow peaks in NaCl are proportional to the initial numbers N_j of defects which were trapped at the corresponding traps T_j , prior to the rise of the glow peaks. These facts enable us to substitute the TL intensities for the numbers of defects, N_j . The dependence of N_j on the wavelength and on the dose of the exciting uv radiation has been formulated by Eqs. (20) and (21). Numerical methods were applied for the analysis of these expressions in the present case of NaCl. Computations were performed for the glow peaks of 102, 186, 213, 250, and 303 K. An attempt was made to fit function (21) to the experimentally measured dose dependence of the various glow peaks. Values of the absorption coefficient were taken from the literature for these computations.⁸ In order to achieve a satisfactory fit, the existence of an additional trap of high trapping probability had to be assumed. A best fit of the function (21) with the experimental dose dependence of the 102-, 213-, and 250-K glow peaks is given by the solid curves a, b, and c in Fig. 6. No satisfactory fit could be achieved for the 303-K glow peak. It may be noted that this glow peak behaved also in other respects differently; as mentioned, it was very sensitive to the pretreatment of the sample and was the sole glow peak that could be excited by both, ionizing and nonionizing uv light. It therefore appears that this glow peak is due to a different process.

The theoretical dose dependence of the normal-

ized number of defects N_j/M_{0j} trapped at the hypothetical trap is shown by curve d of Fig. 6. This curve reveals a linear dose dependence for relatively low doses and a sublinear dependence for higher doses, whereas curves a-c show superlinear dose dependence. Although the existence of such an additional trap had *a priori* been only hypothetically assumed, we found the measured dose dependence of the 350-K glow peak to fit curve d of Fig. 6. Since the 350-K peak appearing in the glow curves was partly overlapped by the stronger 303-K peak, the contribution of this 303-K peak to the total luminescence intensity at 350 K had to be taken into account. This contribution was estimated to be about 10% of the peak intensity at 303 K. In Fig. 5, a comparison is shown between the measured dose dependence of the glow-peak intensity at 350 K (represented by squares) and that of the hypothetical glow peak (represented by crosses) taking into account the above-mentioned contribution of the 303-K peak. The apparent agreement indicates that the trap connected with the 350-K glow peak is probably the one responsible for the appearance of the superlinear dose dependence in other glow peaks of NaCl.

Superlinear dependences of TL intensities on the dose of the exciting radiation were previously observed and explained in different ways for certain cases.⁸ These explanations appeared not to fit our case of NaCl.

An additional check for the validity of Eq. (21) was provided by the TL excitation spectra. The various parameters of Eqs. (20) and (21) were found from the best fit of this function (for a given exciting wavelength) with the experimentally measured dose dependence. With the aid of these values, the theoretical dependences of the glow-peak intensities on the exciting wavelengths were computed for a given radiation dose. Theoretical excitation spectra, as achieved by this method, are shown by the solid curves in Fig. 4. These curves fit well the measured excitation spectra in the region of the exciton band for $\lambda > 158$ nm. The deviations for shorter wavelengths may be due to the very steep increase of the absorption coefficient (μ) and to the fact that the values of μ were previously extrapolated⁸ for $\lambda > 158.5$ nm. They may also be connected with the fact that in this region of very high absorption all excitation processes are practically restricted to an extremely thin surface layer, where the distribution of traps is probably quite different from that in the bulk.

The agreement between the experimental excitation spectra and dose dependence and the theoretical functions supports, evidently, the proposed competition model. This model can be used to explain superlinear as well as linear and sublinear dose dependences.

¹N. Kristianpoller and M. Israeli, *Phys. Rev. B* **2**, 2175 (1970); M. Israeli and N. Kristianpoller, *Phys. Status Solidi* **45**, k29 (1971).

²N. Kristianpoller and M. Israeli, *Phys. Status Solidi* **47**, 487 (1971).

³H. N. Hersh, *Phys. Rev.* **148**, 928 (1966); D. Pooley, *Proc. Phys. Soc. (London)* **87**, 245 (1966); **87**, 257 (1966).

⁴M. Israeli and N. Kristianpoller, in *Proceedings of the International Conference on Color Centers in Ionic Crystals*, Reading, 1971, H165 (unpublished).

⁵See, e.g., F. T. Goldstein, *Phys. Status Solidi* **20**, 379 (1967); Y. Farge, *J. Phys. Chem. Solids* **30**, 1375 (1969).

⁶T. Miyata and T. Tomiki, *J. Phys. Soc. Japan* **21**, 395 (1966).

⁷N. Kristianpoller, M. Israeli, and R. Chen (unpublished).

⁸See, e.g., A. Halperin and R. Chen, *Phys. Rev.* **148**, 839 (1966); M. Israeli and N. Kristianpoller, *Solid State Commun.* **7**, 1131 (1969); E. T. Rodine and P. L. Land, *Phys. Rev. B* **4**, 2701 (1971).

PHYSICAL REVIEW B

VOLUME 6, NUMBER 12

15 DECEMBER 1972

Ionic-Thermocurrent Study of Rare-Earth-Doped CaF_2 and SrF_2 †

J. Wagner

Physics Department, Medical Physics Laboratory, University of Wisconsin, Madison, Wisconsin 53706

and

S. Mascarenhas

Physics Department, Escola de Engenharia, São Carlos, São Paulo, Brazil

(Received 8 June 1972)

The reorientational properties of CaF_2 doped with the rare earths (RE) cerium, praeosodymium, samarium, europium, and terbium were studied using the technique of ionic thermocurrents (ITC). The reorientational energies of the RE- F^- -interstitial complex formed were found to increase with increasing ionic radius of the impurity rare-earth ion, increasing more rapidly for the larger ions. All energies were much less than the free F^- -interstitial activation energy. The preexponential factors were larger than the normal vibrational frequencies in the CaF_2 lattice and perhaps reflect the tight-binding nature of the complex. A natural Brazilian fluoride sample known to contain aluminum fit nicely with the other data. Oscillator strengths for the $4f \rightarrow 5d$ optical transition for the RE ion in tetragonal symmetry in the CaF_2 lattice were determined for Ce, Pr, and Tb using ITC and optical-absorption data. ITC runs on $\text{SrF}_2:\text{Eu}$ were also made. The peak structure observed was more complicated. Three peaks were separated and their activation energies and frequency factors determined.

I. INTRODUCTION

The measurement of reorientational properties of electric dipolar complexes in insulators has become simpler and more direct with the introduction of the ionic-thermocurrent (ITC) technique by Bucci, Fieschi, and Guidi in 1966. Before the introduction of this method, dielectric loss, NMR, tracer studies, and ionic conductivity were the main techniques for investigating ionic motion in ionic solids. Since its introduction, ITC has been used to determine reorientational properties and monitor other phenomena of various impurity complexes in a good number of alkali halides.¹⁻⁴ In almost all cases, these results have been in good agreement with the results obtained using other methods.⁵

Motional effects in the fluorite lattice have not proved as straightforward. A common type of electric dipole complex found in CaF_2 involves a trivalent positive ion such as a rare earth (RE) which enters the lattice substitutionally for the

calcium and the charge-compensating fluorine interstitial ion. (The interstitial position in the fluorite lattice is the vacant body center of the cube of F^- that is adjacent to a cube of F^- with the cation at its center.) Owing to the Coulomb attraction of the two ions one would expect them to be bound at sufficiently low temperatures; therefore, the complex will possess a permanent electric dipole moment. A common symmetry of this type of complex is tetragonal, with the F_i^- occupying the nearest-neighbor interstitial position to the $3+$ cation. Many other types of dipolar complexes may be thought of and formed in this lattice through the proper introduction of certain impurities, but in this paper we will only be interested in complexes involving trivalent positive ions and fluorine interstitials.

Until recently, measured values of reorientational parameters and just simple diffusion parameters in rare-earth- or trivalent-positive-ion-doped CaF_2 have diverged by 50–100%,⁶⁻⁸ in great contrast to the results in alkali halides. Lately, things have been improving. There have been re-